Journal of
Mechanical
Science and
Technology

Journal of Mechanical Science and Technology 21 (2007) 2237~2243

An experimental study on the AC electroosmotic flow around a pair of electrodes in a microchannel

Hyeung Seok Heo, Sangmo Kang and Yong Kweon Suh*

Department of Mechanical Engineering, Dong-A University, 840 Hadan-dong, Saha-gu, Busan 604-714, Korea

(Manuscript Received December 30, 2006; Revised March 28, 2007; Accepted July 6, 2007)

Abstract

This paper presents an experimental study on the AC electroosmotic flow in a microchannel having a pair of rectangular electrodes on the bottom wall with narrow gap. The microchannel was made of PDMS (Polydimethylsiloxane) and the electrodes of ITO (Indium Tin Oxide). The electrodes were arranged such that the electric field is mainly perpendicular to the channel's longitudinal direction, thus creating a transversal secondary flow. The primary flow was driven by a pressure force through the fluid-level difference on both reservoirs of the channel. To measure the velocity distributions around the electrodes, we used a micro-PTV (particle tracking velocimetry) technique. We find that on the surface of the electrodes the flow velocity caused by the AC electroosmosis is directed from the electrode edge toward the side wall of the channel, and the maximum crosswise velocity occurs at the frequency 120Hz. A smooth profile of the crosswise velocity component along a vertical line was successfully obtained from the present experimental technique, and it shows a flow reversal due to the mass conservation principle.

Keywords: AC electroosmosis; Microchannel; ITO (Indium Tin Oxide) glass; Micro-PTV

1. Introduction

In order to control fluid flows and to manipulate bio-particles in micro devices, we use in many cases electrokinetic forces leading to phenomena peculiar to microfluidics, such as electroosmosis, electrophoresis, and di-electrophoresis. Here, the former two phenomena are achieved by applying DC on both ends of a microfluidic device, usually a microchannel. The electroosmosis is the fluid flow caused by the accumulation of charges on the EDL (electric double layer) of channel walls and their motions in response to the externally applied electric field. The electrophoresis corresponds to the motion of particles spread within the channel also due to the charge accumulation around the EDL of the surface of the particles themselves. The third phenomenon, di-electrophoresis, is induced by the non-zero gradient of the electric field in the microfluidic device dictated by the embedded electrodes. There are numerous examples of particle assembly or separation achieved by the application of di-electrophoretic effect (e.g. Fiedler et al. [1], Schnelle et al. [2] and Yu et al. [3]). In di-electrophoresis, particles can be accumulated around or separated from the edge of the electrodes depending on the surface nature of the particles and the frequency of the applied (usually AC) electric field.

On the other hand, very recently, applying the concept of AC electroosmosis to particle manipulation has been emerging. The response of EDL to the AC is more interesting and of course more dynamic than DC. We can use the forcing frequency as another control parameter and so it is more feasible in its application. Further, the electrode life becomes longer with AC due to the suppression of the electrochemical reactions (e.g., Islam and Wu [4]). Use of metal electrodes together with AC in controlling particle assembly in small devices has been reported. Trau et al.

*Corresponding author. Tel.: +82 51 200 7648
E-mail address: yksuh@dau.ac.kr

[5] showed the long-range attraction of 2μm-size particles on ITO electrodes, and they attributed such a phenomenon to the hydrodynamic force given by the induced charge on the electrode. Green's group [6, 7] reported separation of sub-micrometer particles on the array of electrodes, and they conjectured that heat generation and subsequent gradient of the conductivity and permittivity of the medium may induce a hydrodynamic force which results in particle migration. One year later, they introduced the concept of AC electric-field induced flow and electrode polarization to explain their experimental findings and proposed a simple capacitor model to verify the magnitude of the measured velocity. However, the predicted velocity turned out to be far greater than the measured one. Another research group [8] attempted to fit the data of the Green's group and their theoretical model [9] without success. Later, Green et al. [10] refined their capacitor model by introducing another parameter considering the effect of potential drop across the compact (Stern) layer. Detailed explanation for the mechanism of the steady-flow occurrence in the AC electroosmosis can be found from Green et al. [10] and Wu et al. [11].

Extensive experimental evidence of AC electroosmosis has been reported in association with the particle migration and assembly. Wong et al. [12] fabricated a circular electrode surrounded by a circular strip of counter electrode and used PIV to measure the fluid velocity provided by the AC electroosmosis. The measured velocity shows its dependence on the frequency and the electrolyte concentration. They also demonstrated the trapping of DNA molecules. Brown and Meinhart [13] also conducted a DNA-concentration experiment with a very similar electrode arrangement as Wong et al. [12]. Their numerical results are, however, two orders of magnitude greater than the measured ones, and the predicted optimum frequency, at which the velocity becomes maximum, is also more than two orders of magnitude smaller than the experimental results. Several experiments on the evidence of particle aggregation along the center of electrode strips have also been reported [11, 14-16]. Bhatt et al. [17] demonstrated the collection and concentration of latex particles and yeast cells around the patterned electrodes. Wong et al. [18] reviewed the various electrokinetic effects and their application in biotechnology. In most cases, the AC electroosmotic effect is naturally combined with the di-electrophoretic effect in control of the particles (e.g., Hoettges [19] and Gagnon and Chang [20]).

In order to apply the concept of AC electroosmosis to the design of microfluidic devices, we must understand the mechanism of the fluid flow that causes the particle motion. For this, a physical insight as well as mathematical analysis of the fundamental problem on the AC electroosmosis is necessary. Although there have been several experimental evidences of particle assembly around the point on the electrode surface where the electric field is weakest, there are very few results that show satisfactory agreement between the theoretical analysis and the experimental results, regarding the flow velocity. This means that we need to improve the measurement technique and simultaneously we have to construct a theoretical analysis that is accurate enough to possibly provide a simple tool to predict the fluid flow and, subsequently, the particle movement. As a first step to establishing this purpose, we are currently doing theoretical and numerical analysis on the governing equation, the ingredient being the so-called Nernst-Planck equation, and also performing a simple experimental study on the velocity measurement as well as flow visualization for the AC electroosmotic flow around a pair of electrodes within a microchannel. This paper reports the results of the velocity measurement and the flow visualization.

2. Experimental method

2.1 Fabrication of the microchannel

The microchannel to be used in this study is depicted in Fig. 1. A pair of ITO electrodes is attached on the bottom wall in asymmetric configuration with the purpose of attaining efficient mixing in a future study.

Fig. 2 illustrates the process of fabrication of the microchannel. The thickness of the ITO film deposited is 200nm. The photoresist was first spin-coated

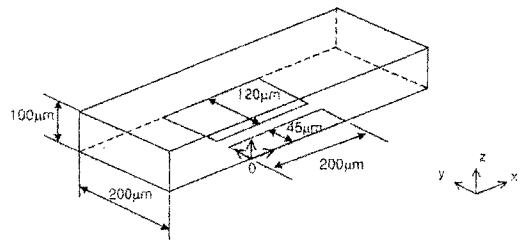

Fig. 1. Geometry and coordinate system of the microchannel; the origin of the coordinates is at the left-low corner of the smaller electrode as indicated by "O".

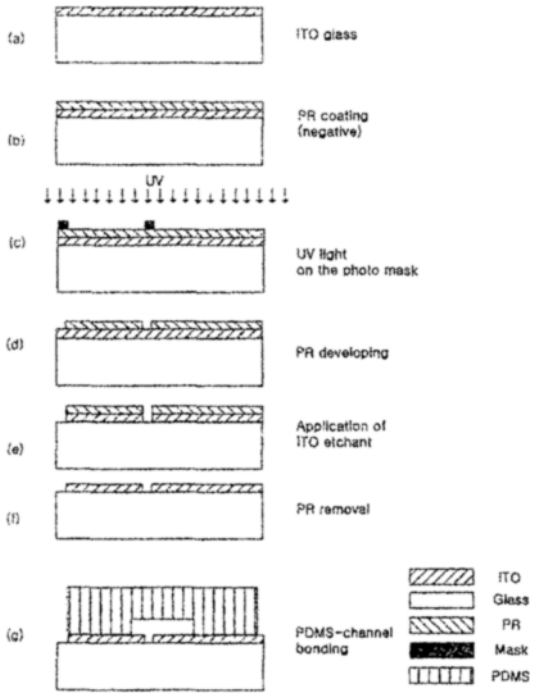

Fig. 2. Procedure for the fabrication of the microchannel with ITO electrodes.

on the ITO-coated glass {Fig. 2(a), (b)} and formed to accommodate the ITO electrodes {Fig. 2(c), (d)}. The ITO layer was then etched with an HNO_3/HCl solution {Fig. 2(e)}. Next, PR removal was used to remove the photoresist {Fig. 2(f)}. On the other hand, a molding master of the microchannel, 100μm high, was patterned on the silicon wafer by use of Deep-RIE (Deep Reactive Ion Etching). The PDMS layers were fabricated by pouring a degassed mixture of Sylgard 184 silicone elastomer (DC-184A) and curing agent (DC-184B) (10:1) onto a molding master, followed by curing for at least 1 hour at 70°C. The cured PDMS was separated from the molding, and holes, to be connected to the reservoirs, were made at the end of each channel by using a 2-mm circular punching device. Strong bonding was made for the PDMS and glass substrate by using a high frequency generator (plasma generator, BD-10A) {Fig. 2(g)}. After plasma generator treatment, $-CH_3$ of the PDMS surface was replaced with H_2O and CO_2. As a result, Si-O-Si covalent bonding occurred between the glass substrate and PDMS. More detailed explanation is given as follows. The formula for PDMS is $-O-Si(CH_3)_2$. This can be made hydrophilic by exposing it to plasma. Exposure to plasma introduces silanol (Si-OH) groups, and destroys the methyl ($Si-CH_3$) groups. These silanol groups then condense with appropriate groups on another surface when the two layers are brought into conformal contact. For PDMS and glass, this reaction yields Si-O-Si bonds after loss of water. These covalent bonds form the basis of a tight seal.

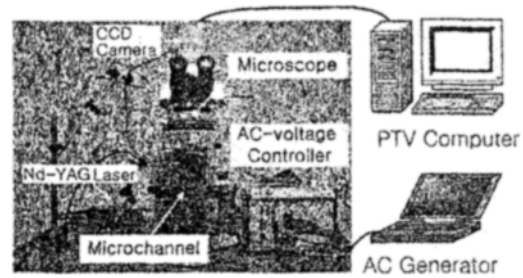

Fig. 3. Schematic diagram of the micro PTV system and experimental set-up.

2.2 PTV system to measure the velocity field

A schematic diagram of the micro PTV system and the experimental setup is shown in Fig. 3. The micro PTV system consists of a microscope (BX51, Olympus), an Nd-YAG laser (532 nm, 800 mW) or a halogen lamp and an AC-voltage controller (PXI-6733, National Instruments). The specification of the objective lens used is M = 20×, 40×, NA = 0.45, 0.60, and the focal depth 11.8 μm, 6.2 μm, respectively. The laser beam illuminates the micro-channel to excite fluorescence particles.

As the working fluid, DI water was used. As the tracing particles, we mixed electrically neutral fluorescence particles of about 1 μm mean diameter (Molecular Probes) in the volume fraction of 50%. The particles were excited at 540 nm by the laser and emitted light with a 560 nm peak. A 550 nm high-pass filter was used to obtain clear fluorescent particle images excluding the scattered laser light emitted from the particles located out of the focal plane. The flow images were captured with a CCD camera (CoolSNAP cf mono, Photometrics) having a 700 × 520 array of square pixels with 12-bit intensity resolution. A 0.5× demagnifying lens was inserted into the optical path between the CCD camera and the microscope to enlarge the field of view. LabVIEW was used to synchronize the image acquisition with the AC-voltage controller. The velocity was obtained by using a simple PTV technique. We also employed a PTV technique using volumetric images and a defocusing method, but this will be explained when the

corresponding results are presented.

The experiment was performed in two stages. In the first stage, no electric voltage was applied to the electrodes, and the fluid was driven only by the application of the pressure force. Motion of particle on the central plane z = 50 μm was visualized by using the objective lens of M = 20× and NA = 0.45 and the laser. The focal depth of this lens was about 12μm. The visualized images were then used to measure the velocity of particles on this plane. The velocity profile obtained in the first experimental stage was used for validation purposes. In the second stage, we conducted experiments for the microchannel flow driven by the AC electroosmosis. Frequency applied in this experiment ranges from 20 Hz to 500 Hz. (At 10 Hz the particles showed vibration and so it was assumed that the results should be unreliable.) The AC voltage applied between the two ITO electrodes was 2V (peak-to-peak). To avoid the particles' adhering to the electrodes, we also applied simultaneously a small unknown pressure gradient (the same amount was applied as for the 1st stage) so that the fluid particles were always moving even when the AC was not applied. During the experiment, the pressure gradient was decreasing slowly due to level change at both reservoirs, and it was found that the total pressure drop during the whole process of the experiment was almost 20%. Since we are interested mainly in the crosswise velocity component around the electrodes not the longitudinal one, the variation in the pressure drop and the subsequent variation in the longitudinal velocity component was not taken to be serious.

3. Experimental results and discussion

First, we checked the validity of the given PTV system by measuring the fluid velocity on the channel center-plane $z = 50$ μm. Presented in Fig. 4 is a comparison of the velocity profile obtained from analytical formula and that obtained from the present PTV measurement. The velocity scale of the analytical profile is arbitrary because the pressure gradient applied in our experiment is unknown. Therefore, the comparison shown in this figure should be understood as the qualitative not quantitative level. Except for the under-prediction near the centerline $y = 100$ μm, the measured data well follow the theoretical data. Deviation near the centerline may be caused by the particles being positioned off the centerline, due to a rather large focal depth. Control of the flow velocity was made by adjusting the height difference of the

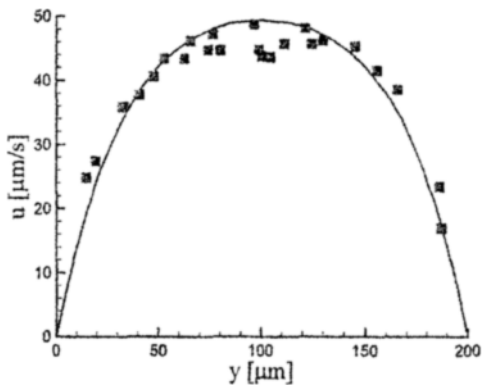

Fig. 4. Comparison of the velocity profiles obtained from theory (solid line) and PTV measurement (symbols) for the case of pressure-driven flow.

free surfaces between the two reservoirs of 10mm in diameter by using a micropipette; when the reservoir size is increased the control becomes easier but it takes a longer time.

Now we present the results obtained from the 2nd-stage experiment. Fig. 5 (a) and (b) show the electroosmotic velocity $V = (u^2 + v^2)^{1/2}$ and the angle $\alpha = \tan^{-1}(v/u)$ of the velocity vector, respectively, measured at the point $(x, y, z) = (100, 95, 9.5)$ μm for various frequency values. As shown in Fig. 5(a), as the frequency is increased, the velocity increases and shows a maximum at the frequency 120 Hz. The velocity is then decreased with the frequency up to 500 Hz. After 500 Hz the velocity magnitude is kept almost constant. This is consistent with the previous study of Green et al. [10] in that their velocity measurement also showed similar trend in the frequency dependence. Fig. 5 (b) shows the direction angle of the velocity vector as a function of the applied frequency. As the frequency is increased, the angle is first increased up to 60 Hz. After that point it shows constant level or abrupt decreasing. Change of the angle indicates that increase of the velocity for the frequency range 20–120 Hz shown in Fig. 5(a) is caused by the increase of the v component in the region above the electrodes. The magnitude of the flow velocity is increased when the applied voltage is increased or when the gap space between the electrodes is decreased. However, during the experiment it was observed that bubbles were generated for excessive setting of these values.

Fig. 6 shows the path lines drawn by the particles on the plane $z = 9.5$ μm obtained for three frequencies. Rectangular boxes indicate the electrodes. It

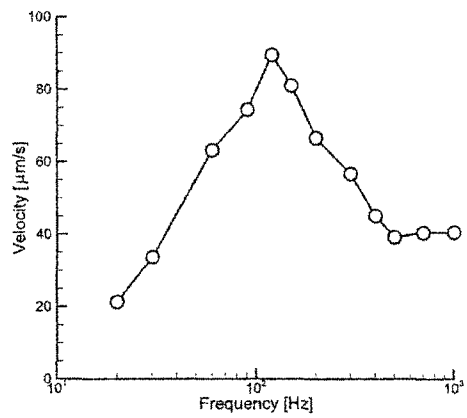

(a)

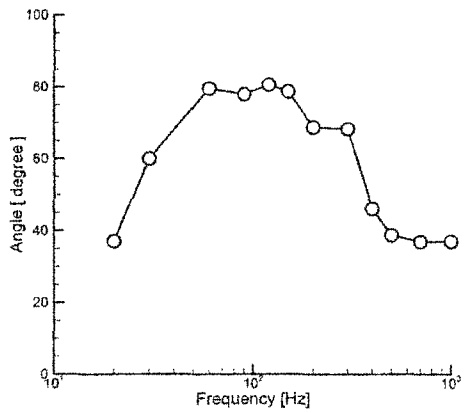

(b)

Fig. 5. (a) Magnitude and (b) phase angle of the of the horizontal velocity vector measured at the point $(x, y, z) = (100, 95, 9.5)$ μm above the larger electrode as a function of the frequency.

shows that particles moving between the two electrodes are attracted to the electrodes and turn abruptly toward the region above the electrodes. The angle of the motion (or vector) is largest near the edge of the electrodes, and this is also consistent with the theoretical prediction given by previous researches (e.g., Green et al. [10]).

Fig. 7 shows distributions of the v velocity along the y -direction on the centerline of electrodes $x = 50$ μm at the height $z = 50$ μm and 9.5 μm at 30Hz. It shows that signs of the velocity components are opposite to each other at the two levels. This indicates that the secondary flows should occur on the channel's cross-section. On the low level, the flow direction will be toward the channel wall, and on the upper level, it will be toward the electrode edges.

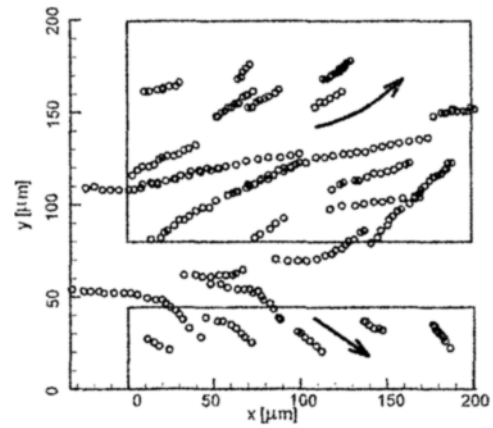

(a)

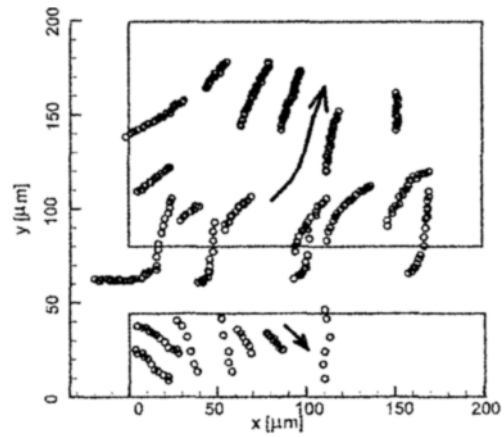

(b)

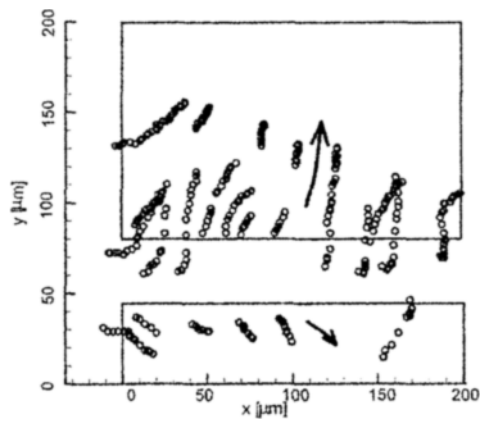

(c)

Fig. 6. Particle path lines measured on the plane $z = 9.5$ μm above the electrodes; (a) 20 Hz, (b) 120 Hz, and (c) 400 Hz.

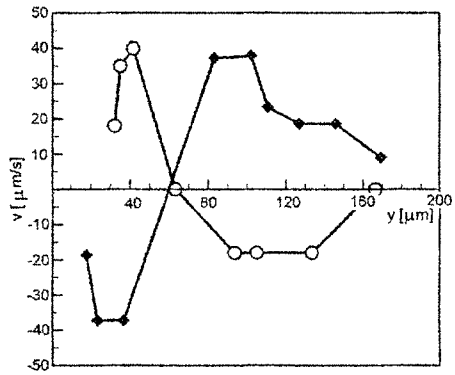

Fig. 7. Distribution of the v-velocity component on the center line of electrodes at the height of 9.5 μm (◆) and 50 μm (○) at 30 Hz.

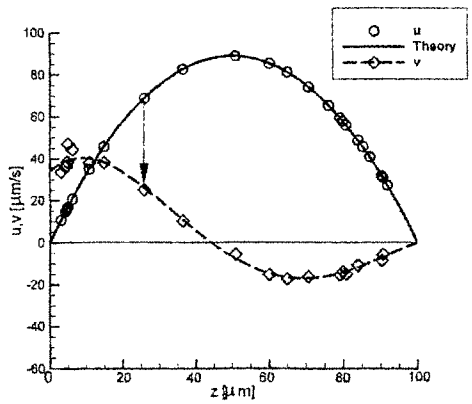

Fig. 8. Distribution of the measured u,v-velocity components (○,◇) along z-direction at the line (x, y)=(100, 110) μm and the streamwise velocity profile obtained from theory (solid line) and the curve (dashed line) fitting the experimental data.

To obtain the velocity profile along the z-direction, we selected a vertical line (x, y) =(100, 110) μm, and shed the halogen light on the bulk region of the channel and recorded the particle trajectories near the selected line. The PTV processing then provided the two components of the velocity, u and v. However due to the scarceness of the particles used in the experiment, there are very few particles passing this point (the line looks a point on the (x, y) plane). Therefore, we included in the measurement the particles passing the region within 5μm in distance. Assuming that the superposition principal holds because the Reynolds number is very low (Re = 0.0133) and that the velocity vectors generated by the AC electroosmosis is purely on the y-z plane, we can write

$$\mathbf{u} = u_P(y,z)\mathbf{i} + v_{AC}(y,z)\mathbf{j} + w_{AC}(y,z)\mathbf{k}$$

where u_P is the pressure-driven velocity and v_{AC} and w_{AC} the AC electroosmotic velocity, respectively. Of course, this assumption should be valid for long electrodes and narrow gap between the pair of electrodes. Then we can use the u-component in predicting the vertical coordinate of the particle by comparing the measured u value with the theoretical profile relevant for the purely pressure-driven case. Since the primary flow profile is close to the parabolic shape, we have two choices as the z-coordinate of the particle. To choose the right position, we applied the defocusing method. The method is based on the fact in optics that the ring radius increases as the particle is moved away from its focal plane. This then provides the rough height of the particle from the use of the correlation between the size of the particle image and the distance from the focal plane (e.g., Wu, et al. [21]).

Fig. 8 shows the u-velocity profiles obtained from the theory (solid line) and u- and v- data obtained from the PTV measurement (symbols) along the z-direction. Because of the forced flow at the electrodes and no-slip condition on the upper wall (i.e., at z=100μm) the v-velocity profile shows both positive and negative flow direction in order to satisfy the continuity equation. This profile may be used in the future when we validate our theoretical or numerical analysis to the AC electroosmotic flow problem in the presence of a pair of electrodes in line with the one treated in this study.

4. Conclusions

We have reported, in this study, the experimental results of the AC electroosmotic flows within a microchannel having a pair of ITO electrodes. By using direct contact of electrodes on the bottom wall in the microchannel we can generate the fluid flows that may have numerous applications, such as mixing and particle assembly in bio-MEMS. We can summarize our important findings in this study as follows.

(1) On the surface of the electrodes, the crosswise velocity component caused by the AC electroosmotic effect is directed from the electrode edge toward the side wall of the channel, being consistent with the previous studies.

(2) In our channel configuration, the maximum crosswise velocity occurs at the frequency 120Hz.

(3) We have developed an experimental technique to measure the velocity profile along a vertical line by using the defocusing method and by comparing one of the velocity components (u-component in this study) and the corresponding theoretical curve.

(4) The profile of the crosswise flow velocity component, which is driven by the AC electroosmotic effect from the electrodes, shows a flow reversal due to the principle of mass conservation.

Acknowledgments

This work was supported by the Korea Science and Engineering Foundation(KOSEF) through the National Research Lab. Program funded by the Ministry of Science and Technology (No. 2005-01091).

References

[1] S. Fiedler, S. G. Shirley, T. Schnelle and G. Fuhr, Dielectrophoretic sorting of particles and cells in a microsystem, *Anal. Chem.* 70 (1998) 1909-1915.

[2] T. Schnelle, T. Muller, S. Fiedler and G. Fuhr, The influence of higher moments on particle behavior in dielectrophoretic field cages, *J. Electrostatics.* 46 (1998) 13-28.

[3] C. H. Yu, J. Vykoukal, D. D. Vykoukal, J. A. Schwartz, L. Shi and P. T. C. Gascoyne, A three-dimensional dielectrophoretic particle focusing channel for microcytometry applications, *J. Microelectromechal Syst.* 14 (3) (2005) 480-487.

[4] N. Islam and J. Wu, Microfluidic transport by AC electroosmosis, *J. Phys.* Conf. Series. 34 (2006) 356-361.

[5] M. Trau, I. A. Savile and Aksay, Assembly of colloidal crystals at electrode interfaces, *Langmuir.* 13 (1997) 6375-6381.

[6] N. G. Green and H. Morgan, Separation of submicrometer particles using a combination of dielectrophoretic and electrohydrodynamic forces, *J. Phys. D: Appl. Phys.* 31 (1998) 25-30.

[7] A. Ramos, H. Morgan, N.G. Green and A. Castellanos, AC Electrokinetics: a review of forces in microelectrode structures, *J. Phys. D: Appl. Phys.* 31 (1998) 2338-2353.

[8] M. Scott, K. V. I. Kaler and R. Paul, Theoretical model of electrode polarization and AC electroosmotic fluid flow in planar electrode arrays, *J. Colloid and Interface Sci.* 238 (2001) 449-451.

[9] M. Scott, R. Paul and K. V. I. Kaler, Theory of frequency-dependent polarization of general planar electrodes with zeta potentials of arbitrary magnitude in ionic media, *J. Colloid and Interface Sci.* 230 (2000) 377-387.

[10] N. G. Green, A. Ramos, A. Gonzalez, H. Morgan and A. Castellanos, Fluid flow induced by nonuniform AC electric fields in electrolytes on microelectrodes. III. observation of streamlines and bumerical simulation, *Phys. Rev. E.* 66 (2002) L25-L30.

[11] J. Wu, Y. Ben, D. Battigelli and H. -C. Chang, Long-range AC electroosmotic trapping and detection of bioparticles, *Ind. Eng. Chem. Res.* 44 (2005) 2815-2822.

[12] P. K. Wong, C. -Y. Chen, T. -H. Wang and C. -M. Ho, Electrokinetic Bioprocessor for concentrating cells and molecules, *Anal. Chem.*, 76 (2004) 6908-6914.

[13] M. R. Brown and C. D. Meinhart, AC electroosmotic flow in DNA concentrator, *Microfluid Nanofluid*, DOI 10.1007/s10404-006-0097-4. (2006)

[14] H. Zhou, L. R. White and R. D. Tilton, Lateral Separation of Colloids or Cells by Dielectrophoresis Augmented by AC Electroosmosis, *J. Colloid and Interface Sci.* 285 (2005) 179-191.

[15] J. Wu, Y. Ben and H. -C. Chang, Particle detection by electrical impedance spectroscopy with asymmetric-polarization AC electroosmotic trapping, *Microfluid Nanofluid.* 1 (2005) 161-167.

[16] M. Lian, N. Islam and J. Wu, Particle line assembly/patterning by microfluidic AC electroosmosis, *J. Phys: Conf. Series.* 34 (2005) 589-594.

[17] K. H. Bhatt, S. Grego and O. D. Velev, An AC electrokinetic technique for collection and concentration of particles and cells on patterned electrodes, *Langmuir.* 21 6603-6612.

[18] P. K. Wong, T.-H. Wang, J. H. Deval and C.-M. Ho, Electrokinetics in micro devices for biotechnology applications, *AIEEE/ASME Trans. Mechatronics.* 9 (2) (2004) 366-376.

[19] K. F. Hoettges, M. B. McDonnell and M. P. Hughes, Use of combined dielectrophoretic /electro-hydrodynamic forces for biosensor enhancement, *J. Phys. D: Appl. Phys.* 36 L101-L104.

[20] Z. Gagnon and H.-C. Chang, Aligning fast alternating current electroosmotic flow fields and characteristic frequencies with dielectrophoretic traps to achieve rapid bacteria detection, *Electrophoresis.* 26 (2005) 3725-3737.

[21] M. Wu, J. W. Roberts and M. Buckley, Three-dimensional fluorescent particle tracking at micron-scale using a single camera, *Exp. Fluids.* 38 (2005) 461-465.